

DENSE GAS PROPERTIES IN ARP 220


Jazeel H. AZEEZ¹

Al-Nahrain University, College of Science, Department of Physics, Iraq

Abstract

Studying dense gas is of fundamental importance for understanding star formation and galaxy evolution. We present data from the Atacama Large Millimeter/Submillimeter Array (ALMA) for the dense molecular gas tracers HNC (hydrogen isocyanide) with transition $J = 2-1$, CS (carbon monosulfide) with transition $J = 4-3$, and CO (carbon monoxide) with transition $J = 6-5$. We studied some properties of dense gases to find their effect on star formation in Arp 220 galaxy. We identify Arp 220 into two regions in which we reveal emission from every one of the three molecules, including the east and west nuclei. We calculate the ratios of $L_{\text{HNC}}/L_{\text{CO}}$, $L_{\text{CS}}/L_{\text{CO}}$, and $L_{\text{CS}}/L_{\text{HNC}}$ at a sub-arcsecond scale. The ratios of $L_{\text{HNC}} / L_{\text{CO}}$ and $L_{\text{CS}} / L_{\text{CO}}$ represent fractions of the dense molecular gas. The values of these ratios are found equal to (0.31, 0.67) and (0.15, 0.31) in the west and east nuclei, respectively. We detect that these ratios are greater in the east nucleus than in the west nucleus. We also calculated the star formation efficiency ($\text{SFE}_{\text{dense}}$), which is the rate of star formation per unit dense gas mass at a sub-arcsecond scale. We found that this galaxy has a long depletion time and low $\text{SFE}_{\text{dense}}$ compared to the global scale.

Keywords: Galaxy, Arp 220, Dense Gas, ALMA.

 <http://dx.doi.org/10.47832/2717-8234.10.2>

¹  jazeelhussein@yahoo.com, <https://orcid.org/0000-0002-4066-6443>

Introduction

High-dense gases carry out a significant part in the physics of Ultra Luminous Infrared Galaxies (ULIRGs), leading to exciting starbursts and perhaps providing the fuel for an active galactic nucleus (AGN)[1*]. The molecular line emissions radiating from the nucleus of the galaxy give knowledge about the actual properties of the galaxy. Furthermore, it can give us an understanding of the procedure affecting the gases within the nuclei, like the formation rate of the star. Although CO has been the most widely recognized molecular gas tracer because of its luminosity and a significantly larger presence in Giant Molecular Clouds (GMCs), it is perhaps not the best tracer for the star-forming molecular gas. HCN [2], CS [3], HNC [4], and HCO⁺ [5], are dense gas tracers that may be used to investigate the molecular gas that is most closely connected to star formation. As a result, these lines may be used to investigate the distribution of dense molecular gas inside a system and restrict the relative percentage of dense gas from one region to the next and the relative importance of physical laws like mechanical heating. Baan [6] displayed data from some line emissions such as CO, HCN, HNC, HCO⁺, CN, and CS in a group of about 37 ULFIRGs and 80 extra sources gathered from the literature to estimate the physical nature of the nuclear disc and its response to changing nuclear performance. However, it is still unclear how molecular gas clouds' characteristics influence their ability to create stars. Because denser gas pockets are more prone to collapse and collapse more quickly, a substantial relationship between gas density and star formation is predicted.

Arp 220 is a close system in the late stages of a merging galaxy with massive ongoing star formation between the two nuclei. These nuclei are very close to each other. They don't appear to be heavily distorted yet. Hence, the two major places are still adequately far away from one another. The emission lines with high-density gas tracers precisely detect the ISM of the two nuclei [7]. In this paper, a high density gas tracer such as HNC and CS is used in Arp 220 by ALMA to study some dense gas properties at a sub-arcsecond scale and to see how this dense molecular gas affects the process of star formation. The following is a summary of the manuscript: Part 2 goes through the data description. Part 3 describes the results, including how to calculate the luminosity, ratio of dense gases, and star formation efficiency, as well as how to interpret the results. Part 4 detailed our findings and conclusions.

1. Data Description

This paper presents two molecular line emissions and HNC (2-1), CS (4-3) of Arp 220. ALMA (band 5) Science Verification Cycle-0 data for Arp 220 were obtained. This data was taken with 12 antennae in a configuration providing a total of 30 m ~ 480 m baselines on July 16th, 2016. With Briggs weighting, the synthesized beam measures 0.7" × 0.6". The robust parameter is set at 0.5. Arp 220's two cores are therefore clearly resolved. The data were made public at <https://bulk.cv.nrao.edu/alldata/sciver/Arp220/>. We combined these data with previously published CO (6-5) data from [8]. The descriptions of these three molecular lines are listed in Table 1. The integrated intensity maps of CO (6-5), HNC (2-1), and CS (4-3) are shown in Figure 1.

Table 1: Flux Density Measurements in Arp 220

Region	Right Ascension (J2000)	Declination (J2000)	$S_{\text{HNC}(2-1)}$ (Jy.km/s)	$S_{\text{CS}(4-3)}$ (Jy.km/s)	$S_{\text{CO}(6-5)}$ (Jy.km/s)
$R_1(\text{West})$	$15^{\text{h}} 34^{\text{m}} 57.299^{\text{s}}$	$23^{\circ} 30' 11''.486$	22.99	12.25	1078.96
$R_2(\text{East})$	$15^{\text{h}} 34^{\text{m}} 57.227^{\text{s}}$	$23^{\circ} 30' 11''.551$	54.13	28.88	1177.80

2. Result and Discussion

2.1 Luminosity of the Dense Gases

In this manuscript, we concentrate on HNC, CS, and CO emissions from the two nuclei in the galaxy Arp 220. Our data cover both nuclei (east and west). We detect abundant dense gas in the east nucleus about more than twice the west nucleus in the HNC and CS emission lines. We sign a circle slot around each of these nuclei in the zero moment map to measure the dense gas flux for each emission line, as shown in figure 1. The radius of each circle is $0.5''$, which is approximately equal to 188 pc. We use a $D = 70.4$ Mpc distance to Arp 220 [8]. We used the measured flux density that we estimated in table 1 to calculate the luminosity of the dense gas in each region at a sub-arcsecond scale by using the following formula [9]:

$$\frac{L}{K \text{ km s}^{-1} \text{ pc}^2} = 3.2546 \times 10^7 \left(\frac{S_{\text{mol}}}{\text{Jy km s}^{-1}} \right) \left(\frac{D_L}{\text{Mpc}} \right)^2 \left(\frac{v_0}{\text{GHz}} \right)^{-2} (1+z)^{-1}$$

Where S_{mol} is the flux density, D_L is the distance, v_0 is the frequency of the transition, and z is the redshift, which is equal to 0.01813. In our interferometric map, the total luminosity from the two nuclei (west and east) for the CO emission line is $L_{\text{CO}} = 4.42 \times 10^8 K \text{ km s}^{-1} \text{ pc}^2$ and $4.83 \times 10^8 K \text{ km s}^{-1} \text{ pc}^2$, respectively. Whereas, the total HNC luminosity over the same region are $L_{\text{HNC}} = 1.38 \times 10^8 K \text{ km s}^{-1} \text{ pc}^2$ and $3.26 \times 10^8 K \text{ km s}^{-1} \text{ pc}^2$ respectively. Lastly, the total CS luminosity from the two nuclei is $L_{\text{CS}} = 0.64 \times 10^8 K \text{ km s}^{-1} \text{ pc}^2$ and $1.49 \times 10^8 K \text{ km s}^{-1} \text{ pc}^2$ respectively. The luminosity results reveal that the east region has higher emissions than the west region for all dense gases.

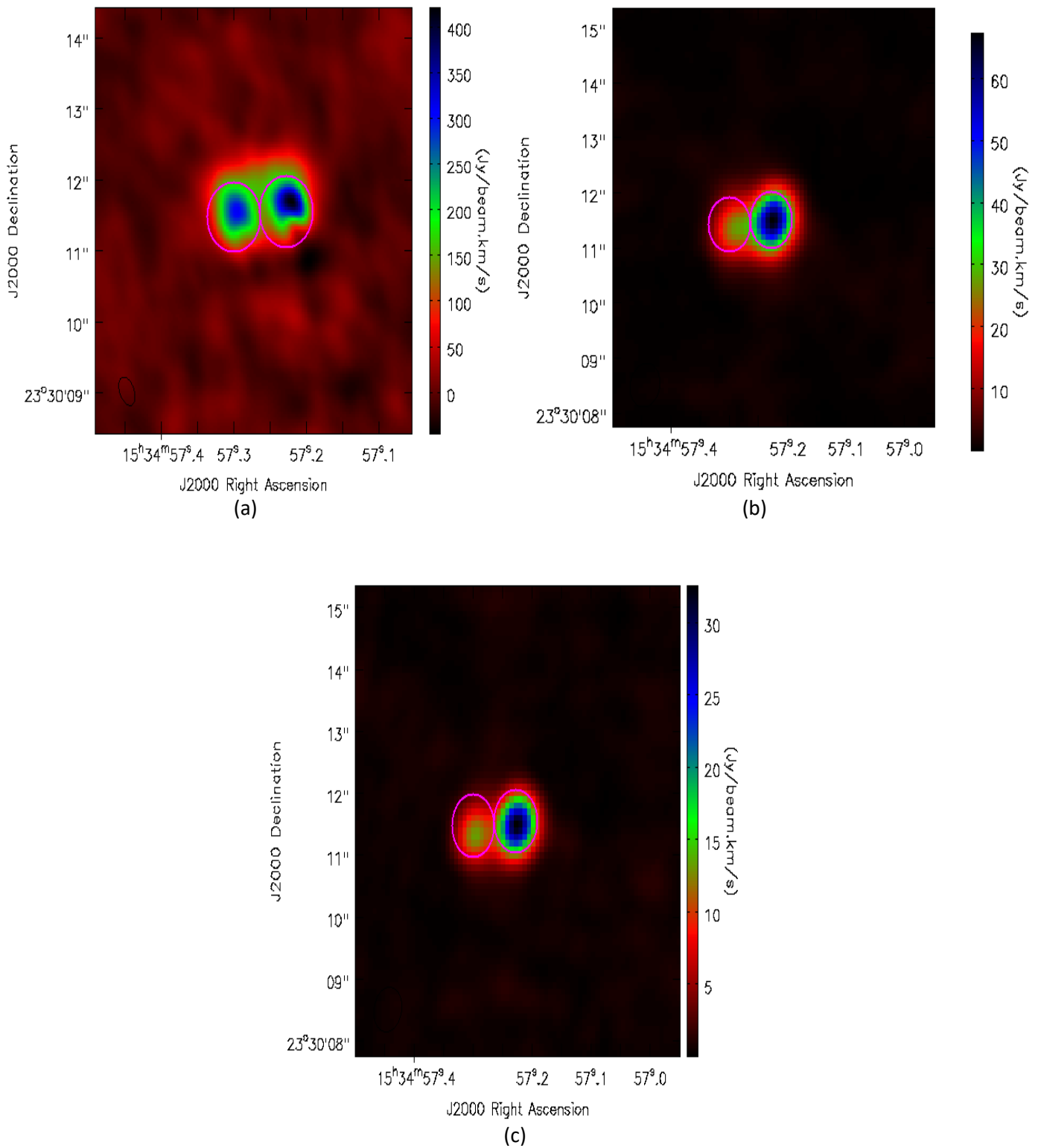


Figure (1): (a) CO (6 - 5), (b) HNC (2 - 1), and (c) CS (4 - 3) moment-0 map from ALMA. The magenta circles show the location of the east and west nuclei.

2.2 Ratio of the Dense Gases

We used the luminosity of the dense gases to find the following ratios of $L_{\text{HNC}} / L_{\text{CO}}$, $L_{\text{CS}} / L_{\text{CO}}$, and $L_{\text{CS}} / L_{\text{HNC}}$. These ratios are listed in table 2. We utilize the ratios of $L_{\text{HNC}} / L_{\text{CO}}$ and $L_{\text{CS}} / L_{\text{CO}}$ as indicators for the density of gas fraction over the two nuclei in Arp 220. Interestingly, the values of these ratios in the west nucleus are about half the values of these ratios in the east nucleus. Whereas the ratio of $L_{\text{CS}} / L_{\text{HNC}}$ in the two nuclei is equal. We argued that the decreased dense gas fraction in the west nucleus is due to the HNC (2 – 1) and CS (4 – 3) emissions not precisely coincident with CO (6 – 5) emissions in this nucleus.

Table 2: Luminosity ratio for the two nuclei in Arp 220

Region	$L_{\text{HNC}(2-1)} / L_{\text{CO}(6-5)}$	$L_{\text{CS}(4-3)} / L_{\text{CO}(6-5)}$	$L_{\text{CS}(4-3)} / L_{\text{HNC}(2-1)}$
R ₁ (West)	0.31	0.15	0.46
R ₂ (East)	0.67	0.31	0.46

3.3 Star Formation Efficiency

The majority of research analyzing dense gas and star formation in distant galaxies has used low-resolution measurements (≤ 1.0 kpc) [10, 11]. Dense gas maps with high-resolution measurements are still uncommon. We calculate the efficiency of star formation (SFE_{dense}) in this work, which is the rate of star formation per unit dense gas mass at a sub-arc-second scale (200 pc) ($SFR_{dense} = \frac{SFR}{M_{dense}}$). This efficiency is the inverse of the depletion time (τ_{dep}). We calculate M_{dense} from L_{HNC} by assuming the conversion factor $\alpha_{\text{HNC}} = 10 M_{\odot} (\text{K km s}^{-1} \text{ pc}^2)^{-1}$ [12]. The infrared data (IR) from the Spitzer Space Telescope is used to track the formation of stars. We utilize 24 μm data from the public archive gathered with the MIPS instrument to estimate the amount of star formation hidden by dust. Azeez et al. [13, 14] showed that the star formation rate may be calculated from 24 μm luminosity using the given equation:

$$\frac{\Sigma SFR}{M_{\odot} \text{ yr}^{-1}} = \frac{\nu L_{\nu}[24 \mu\text{m}]}{6.66 \times 10^8 L_{\odot}}$$

Where L_{ν} is the luminosity at 24 μm . The values of the dense gas mass, star formation rate, SFE_{dense}, and depletion time are listed in Table 3. From the above table, we notice that our measurements at < 200 pc resolution within the two nuclei of the LIRG Arp 220 reveal relatively low star formation efficiencies, corresponding to long depletion times of ~0.16–0.32 Gyr for the bulk molecular gas traced by HNC. These values are considered long depletion times [15]. As a result, active galactic centers appear to have fewer IR emissions (and consequently smaller SFR) per unit of dense gas emission at a few hundred pc scale. The low value of SFE_{dense}, less than 200 pc on a global scale, could be attributed to AGN effects. In addition, it can be interpreted as the collision processes between dense gas molecules that might occur at larger scales.

Table 3: Values of dense gas mass, star formation rate, star formation efficiency, and depletion time for the two nuclei in Arp 220

Region	$M_{dense} (M_{\odot})$	$\Sigma_{SFR} (M_{\odot} \text{ yr}^{-1})$	$SFE_{dense} (\text{yr}^{-1}) \times 10^{-9}$	$\tau_{dep} (\text{Gyr})$
R ₁ (West)	1.38	0.44	3.17	0.32
R ₂ (East)	3.26	0.51	1.58	0.16

3. Summary and Conclusion

We present high spatial resolution data of some molecular dense gas tracers: CO (6 – 5), HNC (2 – 1), and CS (4 – 3) for the LIRG Arp 220 from ALMA to explore several dense gas features at the sub-arcsecond scale and investigate how this dense molecular gas affects the star formation process. The following is a summary of the key findings:

- We have calculated the luminosity of the three dense gases (L_{CO} , L_{HNC} , and L_{CS}) in the east and west nuclei of Arp 220. For all dense gases, the luminosity data shows that the east region emits more than the west region.

- We calculate the ratios of L_{HNC} / L_{CO} , L_{CS} / L_{CO} , and L_{CS} / L_{HNC} at sub-arcsecond scale. Where the ratios of L_{HNC} / L_{CO} and L_{CS} / L_{CO} are indicators for the dense gas fraction over the two nuclei in Arp 220. In the west and east nuclei, these ratios are equal to (0.31, 0.67) and (0.15, 0.31), respectively.

- We measured SFR using $24 \mu\text{m}$ data from Spitzer, then we calculated the efficiency of star formation (SFE_{dense}), which is the inverse of the depletion time. The values of this efficiency in the east and west nuclei at the sub arcsecond scale are $(3.17 \text{ and } 1.58) \times 10^{-9} \text{ yr}^{-1}$ respectively, which are considered low values despite the fact that there is a vast reserve of molecular gas obtainable. This means that some mechanisms may obstruct the creation of stars in dense gas. These processes might be caused by the AGN's strong kinetic energy injection, which suppresses star formation.

References

- [1] I. Oteo et al., “High Dense Gas Fraction in Intensely Star-forming Dusty Galaxies”, *The Astrophysical Journal*, vol. 850, pp. 170-179, 2017.
- [2] P. P. Papadopoulos, “HCN versus HCO⁺ as dense molecular gas mass tracers in luminous infrared galaxies”, *The Astrophysical Journal*, vol. 656, pp.792 - 797, 2007.
- [3] T. R. Greve, P. P. Papadopoulos, Y. Gao, and S. J. E. Radford, “Dense Molecular Gas in Extreme Starburst Galaxies –What will we learn from Herschel?”, *ArXiv Astrophysics e-prints*, 2006.
- [4] D. Talbi, Y. Ellinger, and E. Herbst, “On the HCN/HNC abundance ratio: a theoretical study of the H⁺ CNH \leftrightarrow HCN+ H exchange reactions”, *Astronomy and Astrophysics*, vol. 314, pp. 688 – 692, 1996.
- [5] J. Graciá-Carpio, S. García-Burillo, P. Planesas, and L. Colina, “Is HCN a True Tracer of Dense Molecular Gas in Luminous and Ultraluminous Infrared Galaxies?”, *The Astrophysical Journal*, vol. 640, No. 2, pp. L135–L138, 2006.
- [6] W. A. Baan et al., “Dense gas in luminous infrared galaxies”, *Astronomy and Astrophysics*, vol. 477, pp.747–762, 2008.
- [7] W. Baan, “Arp 220 – IC 4553/4: Understanding the system and diagnosing the ISM.” *Proceedings of the International Astronomical Union*, 3(S242), pp.437-445 (2007).
- [8] J.H. Azeez, A.A. Zghair, S.A. Fadhil, and Z.Z. Abidin, “Rotational Velocity and Dynamical Mass for the Nuclear Disk of the ULIRG Arp 220”, *Journal of Physics: Conference Series*, 1829, 2021.
- [9] M. R. P. Schirm, C. D. Wilson, S. C. Madden, and D. L. Clements, “The Dense Gas in the Largest Molecular Complexes of the Antennae: HCN and HCO⁺ Observations of NGC 4038/39 using ALMA”, *The Astrophysical Journal*, vol. 823, pp.87 – 97, 2016.
- [10] S. García-Burillo et al., “Star-formation laws in luminous infrared galaxies, New observational constraints on models”, *Astronomy and Astrophysics*, vol. 539, A8, 2012.
- [11] F. Bigiel et al., “The EMPIRE survey: systematic variations in the dense gas fraction and star formation efficiency from full-disk mapping of M51”, *The Astrophysical Journal Letters*, vol. 822, L26, 2016.
- [12] Y. Gao, and P. M. Solomon, “HCN Survey of Normal Spiral, Infrared-luminous, and Ultraluminous Galaxies”, *The Astrophysical Journal Supplement Series*, vol. 152, no. 1, pp. 63–80, 2004.
- [13] J. H. Azeez, Z. Z. Abidin, C.Y. Hwang, and Z. A. Ibrahim, “Star Formation Law at Sub-kpc Scale in the Elliptical Galaxy Centaurus A as Seen by ALMA”, *Advances in Astronomy*, vol. 2017, 2017.
- [14] J. H. Azeez, Z. Z. Abidin, S. A. Fadhil, and C.Y. Hwang, “Analyzing Interferometric CO(3-2) Observations of NGC 4039”, *Sains Malaysiana*, vol. 51, no. 4, 2022
- [15] M. Querejeta, et al., “Dense gas is not enough: environmental variations in the star formation efficiency of dense molecular gas at 100 pc scales in M 51”, vol. 625, A19, 2019.